Mortar methods with optimized transmission conditions for advection-diffusion problems

Caroline Japhet[1] and Yvon Maday[2]

1 Introduction

In many practical applications in fluid dynamics, a very large range of scales spanning many orders of magnitude are simultaneously present; one possibility to perform an economical and accurate approximation of the solution is to use different discretizations in different regions of the computational domain to match with the physical scales. The mortar element method introduced in Bernardi et al. [1994] allows such a use of different discretizations in an optimal way in the sense that the error is bounded by the sum of the subregion-by-subregion approximation errors without constraint on the choice of the different discretizations. An extension to fluids is given in Achdou et al. [1998]. An alternative and simpler method, the New Interface Cement Equilibrated Mortar (NICEM) method proposed in Gander et al. [2005] and analyzed in Japhet et al. [2013] for an elliptic problem, allows to optimally match Robin conditions on non-conforming grids. An extension to Ventcel conditions is given in Japhet et al. [2014]. The main feature of this approach is that, on each side of the interface, the jump of the Robin or Ventcel condition should be L^2-orthogonal to a well chosen finite element space on the interface (in that case there is no master and slave sides, which makes the method simpler). Thus, it allows to combine different approximations in different subdomains in the framework of optimized Schwarz algorithms which are based on optimized Robin or Ventcel transmission conditions and lead to robust and fast algorithms (see Japhet [1998], Dubois [2007]).

In this paper we extend the NICEM method to advection-diffusion problems. For simplicity we consider the case of Robin conditions.

Université Paris 13, LAGA, UMR 7539, F-93430, Villetaneuse, France. INRIA Paris-Rocquencourt, BP 105, 78153 Le Chesnay, France, japhet@math.univ-paris13.fr · Sorbonne Universités, UPMC Univ Paris 06 and CNRS, UMR 7598, Laboratoire Jacques-Louis Lions, F-75005, Paris, France. Institut Universitaire de France. Brown Univ, Division of Applied Maths, Providence, RI, USA, maday@ann.jussieu.fr

* This work was partially supported by the french LEFE/MANU-CoCOA project.

We first introduce the problem at the continuous level: find u such that

$$\eta u + \nabla \cdot (\boldsymbol{a} u) - \nabla \cdot (\nu \nabla u) = f \quad \text{in } \Omega \tag{1}$$
$$u = 0 \quad \text{on } \partial\Omega, \tag{2}$$

where Ω is a $\mathcal{C}^{1,1}$ (or convex polygon in 2D or polyhedron in 3D) domain of $\mathbb{R}^d$, $d = 2$ or 3, and f is given in $L^2(\Omega)$. We consider a decomposition of Ω into K non-overlapping subdomains: $\overline{\Omega} = \cup_{k=1}^{K} \overline{\Omega}^k$, where Ω^k, $1 \le k \le K$ are either $\mathcal{C}^{1,1}$ or polygons in 2D or polyhedrons in 3D. We suppose that this decomposition is geometrically conforming. Let $\boldsymbol{n}_k$ be the outward normal from Ω^k. Let $\Gamma^{k,\ell} := \partial\Omega^k \cap \partial\Omega^\ell$ denote the interface of two adjacent subdomains. An optimized Schwarz algorithm with Robin transmission conditions for problem (1)-(2) is

$$\begin{aligned} \eta u_k^{n+1} + \nabla \cdot (\boldsymbol{a} u_k^{n+1}) - \nabla \cdot (\nu \nabla u_k^{n+1}) &= f && \text{in } \Omega^k \\ u_k^{n+1} &= 0 && \text{on } \partial\Omega^k \cap \partial\Omega \\ \mathcal{B}_{k,\ell}(u_k^{n+1}) &= \mathcal{B}_{k,\ell}(u_\ell^n) && \text{on } \Gamma^{k,\ell} \end{aligned}$$

where $(\mathcal{B}_{k,\ell})_{1\le k,\ell\le K, k\neq\ell}$ is the Robin transmission operator on the interface between subdomains Ω^k and Ω^ℓ: $\mathcal{B}_{k,\ell}\varphi = \nu\partial_{\boldsymbol{n}}\varphi - \frac{\boldsymbol{a}\cdot\boldsymbol{n}_k}{2}\varphi + \alpha\varphi$ with $\alpha > 0$ given. Following the ideas in Gander et al. [2005], Japhet et al. [2013], we need to introduce a new independent entity representing the flux on the interface, in order to match the Robin conditions on non-conforming grids, and thus the method is of Petrov Galerkin type.

In Sect. 2 we introduce the method at the continuous level. Then in Sect. 3, we present the method in the non-conforming discrete case. The numerical analysis is given in Sect. 4. In Sect. 5 we give the discrete algorithm. In Sect. 6 we show simulations to illustrate the optimality of the method.

2 Definition of the problem

The variational statement of problem (1)-(2) is: Find $u \in H_0^1(\Omega)$ such that

$$\int_\Omega \left(\nu \nabla u \cdot \nabla v + (\eta + \frac{1}{2}\nabla \cdot \boldsymbol{a}) uv + \frac{1}{2}\big((\boldsymbol{a}\cdot\nabla u)v - (\boldsymbol{a}\cdot\nabla v)u\big) \right) dx = \int_\Omega f v dx, \quad \forall v \in H_0^1(\Omega). \tag{3}$$

We suppose that $\nu \ge \nu_0 > 0$ *a.e.* in Ω and $\eta + \frac{1}{2}\nabla\cdot\boldsymbol{a} \ge \eta_0 > 0$ *a.e.* in Ω. Therefore problem (1)-(2) is coercive. We define the space $H_*^1(\Omega^k)$ by

$$H_*^1(\Omega^k) = \{\varphi \in H^1(\Omega^k),\ \varphi = 0 \text{ over } \partial\Omega \cap \partial\Omega^k\}.$$

In order to glue non-conforming grids with Robin conditions, denoting by $\underline{v}$ the K-tuple $(v_1, ..., v_K)$, we introduce the following constrained space,

$$\mathcal{V} = \{(\underline{v}, \underline{q}) \in \left(\prod_{k=1}^{K} H^1_*(\Omega^k)\right) \times \left(\prod_{k=1}^{K} H^{-1/2}(\partial\Omega^k)\right), \\ v_k = v_\ell \text{ and } q_k = -q_\ell \text{ over } \Gamma^{k,\ell},\ \forall k, \ell\}.$$

The following result is an extension of Lemma 1 in Japhet et al. [2013]: problem (3) is equivalent to the following one: Find $(\underline{u}, \underline{p}) \in \mathcal{V}$ such that

$$\sum_{k=1}^{K} \int_{\Omega^k} \left(\nu \nabla u_k \cdot \nabla v_k + (\eta + \frac{1}{2}\nabla \cdot \boldsymbol{a}) u_k v_k + \frac{1}{2}\big((\boldsymbol{a} \cdot \nabla u_k) v_k - (\boldsymbol{a} \cdot \nabla v_k) u_k\big)\right) dx \\ - \sum_{k=1}^{K} {}_{H^{-1/2}(\partial\Omega^k)} < p_k, v_k >_{H^{1/2}(\partial\Omega^k)} = \sum_{k=1}^{K} \int_{\Omega^k} f_k v_k dx, \quad \forall \underline{v} \in \prod_{k=1}^{K} H^1_*(\Omega^k).$$

Being equivalent to the original problem, with $p_k = \nu \frac{\partial u}{\partial \boldsymbol{n}_k} - \frac{\boldsymbol{a} \cdot \boldsymbol{n}_k}{2} u$ over $\partial\Omega^k$ (recall that f is assumed to be in $L^2(\Omega)$ so that $\frac{\partial u}{\partial \boldsymbol{n}_k}$ actually belongs to $H^{-1/2}(\partial\Omega^k)$), this problem is naturally well posed.

Let us describe the method in the non-conforming discrete case.

3 Non-conforming discrete formulation

We first introduce the discrete spaces. Each subdomain Ω^k is provided with its own mesh $\mathcal{T}_h^k$, such that $\overline{\Omega}^k = \cup_{T \in \mathcal{T}_h^k} T,\ 1 \le k \le K$. For $T \in \mathcal{T}_h^k$, let h_T be the diameter of T and h the discretization parameter: $h = \max_{1 \le k \le K} h_k$ with $h_k = \max_{T \in \mathcal{T}_h^k} h_T$. We suppose that $\mathcal{T}_h^k$ is uniformly regular and that the sets belonging to the meshes are of simplicial type (triangles or tetrahedra). Let $\mathcal{P}_M(T)$ denote the space of all polynomials defined over T of total degree less than or equal to M. The finite elements are of lagrangian type, of class $\mathcal{C}^0$. We define on Ω^k the spaces $Y_h^k = \{v_{h,k} \in \mathcal{C}^0(\overline{\Omega}^k),\ v_{h,k|T} \in \mathcal{P}_M(T),\ \forall T \in \mathcal{T}_h^k\}$ and $X_h^k = \{v_{h,k} \in Y_h^k,\ v_{h,k|\partial\Omega^k \cap \partial\Omega} = 0\}$. The space of traces over each $\Gamma^{k,\ell}$ of elements of Y_h^k is denoted by $\mathcal{Y}_h^{k,\ell}$. With each interface $\Gamma^{k,\ell}$, we associate a subspace $\tilde{W}_h^{k,\ell}$ of $\mathcal{Y}_h^{k,\ell}$ in the same spirit as in the mortar element method Bernardi et al. [1994] in 2D or Braess and Dahmen [1998], Ben Belgacem and Maday [1999] for a P_1-discretization in 3D.

More precisely, let $\mathcal{T}$ be the restriction to $\Gamma^{k,\ell}$ of the triangulation $\mathcal{T}_h^k$. In 2D, $\mathcal{T}$ is one-dimensional with vertices $x_0^{k,\ell}, x_1^{k,\ell}, ..., x_{n-1}^{k,\ell}, x_n^{k,\ell}$ and has two end points $x_0^{k,\ell}$ and $x_n^{k,\ell}$. Then $\tilde{W}_h^{k,\ell}$ is the subspace of $\mathcal{Y}_h^{k,\ell}$ of elements that are polynomials of degree $\le M-1$ over both $[x_0^{k,\ell}, x_1^{k,\ell}]$ and $[x_{n-1}^{k,\ell}, x_n^{k,\ell}]$.

In 3D, we suppose that all the vertices of the boundary of $\Gamma^{k,\ell}$ are connected to zero, one, or two vertices in the interior of $\Gamma^{k,\ell}$. We denote by $\mathcal{V}$, $\mathcal{V}_0$, $\partial\mathcal{V}$ the sets of all the vertices of $\mathcal{T}$, the vertices in the interior of $\Gamma^{k,\ell}$, and the vertices on the boundary of $\Gamma^{k,\ell}$ respectively. Let $S(\mathcal{T})$ be the space of piecewise linear functions with respect to $\mathcal{T}$ which are continuous on $\Gamma^{k,\ell}$ and vanish on its boundary. Then $S(\mathcal{T}) =$ span $\{\Phi_a : a \in \mathcal{V}_0\}$ where $\Phi_a,\ a \in \mathcal{V}$ are the finite element basis functions. For $a \in \mathcal{V}$, let $\sigma_a := \{T \in \mathcal{T} : a \in T\}$ denote the support of Φ_a, $\mathcal{N}_a := \{b \in \mathcal{V}_0 : b \in \sigma_a\}$, and $\mathcal{N} := \cup_{a\in\partial\mathcal{V}}\mathcal{N}_a$. Let $\mathcal{T}_c$ be the set of triangles $T \in \mathcal{T}$ which have all their vertices on the boundary of $\Gamma^{k,\ell}$. For $T \in \mathcal{T}_c$, we denote by c_T the only vertex of T that has no interior neighbor. Let $\mathcal{N}_c$ denote the vertices a_T of $\mathcal{N}$ which belong to a triangle adjacent to a triangle $T \in \mathcal{T}_c$. We introduce $\hat{\Phi}_a$ defined as follows: $\hat{\Phi}_a := \Phi_a,\ a \in \mathcal{V}_0 \setminus \mathcal{N},\ \hat{\Phi}_a := \Phi_a + = \sum_{b\in\partial\mathcal{V}\cap\sigma_a} A_{b,a}\Phi_b,\ a \in \mathcal{N} \setminus \mathcal{N}_c$, and $\hat{\Phi}_a := \Phi_{a_T} + = \sum_{b\in\partial\mathcal{V}\cap\sigma_{a_T}} A_{b,a_T}\Phi_b + \Phi_{c_T},\ a = a_T \in \mathcal{N}_c$. The weights are defined by : $A_{c,a} + A_{c,b} = 1$ and $|T_{2,b}|A_{c,a} = |T_{2,a}|A_{c,b}$, for all $c \in \partial\mathcal{V}$ connected to two interior nodes a and b, where $T_{2,a}$ (resp. $T_{2,b}$) denote the adjacent triangle to abc having a (resp. b) as a vertex and its two others vertices on $\partial\mathcal{V}$. For all $c \in \partial\mathcal{V}$ connected to only one interior node a, the weights are $A_{c,a} = 1$ (see Braess and Dahmen [1998]). The space $\tilde{W}_h^{k,\ell}$ is then defined by $\tilde{W}_h^{k,\ell} :=$ span $\{\hat{\Phi}_a,\ a \in \mathcal{V}_0\}$. Then $\tilde{W}_h^k := \prod_{\ell,\ \Gamma^{k,\ell}\neq\emptyset} \tilde{W}_h^{k,\ell}$.

We now define the discrete constrained space as follows:

$$\mathcal{V}_h = \{(\underline{u}_h, \underline{p}_h) \in \left(\prod_{k=1}^{K} X_h^k\right) \times \left(\prod_{k=1}^{K} \tilde{W}_h^k\right),$$
$$\int_{\Gamma^{k,\ell}} ((p_{h,k} + \alpha u_{h,k}) - (-p_{h,\ell} + \alpha u_{h,\ell}))\psi_{h,k,\ell} = 0,\ \forall\psi_{h,k,\ell} \in \tilde{W}_h^{k,\ell},\ \ \forall k, \ell\}.$$

The discrete problem is the following one : Find $(\underline{u}_h, \underline{p}_h) \in \mathcal{V}_h$ such that

$$\begin{aligned}
&\sum_{k=1}^{K} \int_{\Omega^k} \left(\nu\nabla u_{h,k} \cdot \nabla v_{h,k} + (\eta + \frac{1}{2}\nabla \cdot \boldsymbol{a})u_{h,k}v_{h,k}\right) dx \\
&\quad + \sum_{k=1}^{K} \int_{\Omega^k} \left(\frac{1}{2}\big((\boldsymbol{a} \cdot \nabla u_{h,k})v_{h,k} - (\boldsymbol{a} \cdot \nabla v_{h,k})u_{h,k}\big)\right) dx \qquad (4)\\
&\quad - \sum_{k=1}^{K} \int_{\partial\Omega^k} p_{h,k}v_{h,k}ds = \sum_{k=1}^{K} \int_{\Omega^k} f_k v_{h,k}dx, \quad \forall \underline{v}_h = (v_{h,1}, ...v_{h,K}) \in \prod_{k=1}^{K} X_h^k.
\end{aligned}$$

4 Best approximation error

In this part we give best approximation results of $(\underline{u}, \underline{p})$ by elements in $\mathcal{V}_h$ (see Japhet et al. [2013]). We define for any $\underline{p}$ in $\prod_{k=1}^{K} L^2(\partial\Omega_k)$ the norm

$\|\underline{p}\|_{-\frac{1}{2},*} = (\sum_{k=1}^{K}\sum_{\substack{\ell=1\\ \ell\neq k}}^{K} \|p_k\|^2_{H_*^{-\frac{1}{2}}(\Gamma^{k,\ell})})^{\frac{1}{2}}$, where $\|.\|_{H_*^{-\frac{1}{2}}(\Gamma^{k,\ell})}$ stands for the dual norm of $H_{00}^{\frac{1}{2}}(\Gamma^{k,\ell})$ (recall that $H_{00}^{\frac{1}{2}}(\Gamma^{k,\ell})$ is the interpolated space of index $\frac{1}{2}$ between $H_0^1(\Gamma^{k,\ell})$ and $L^2(\Gamma^{k,\ell})$, see Lions and Magenes [1968]).

Theorem 1. *Let us assume that $\alpha h \leq c$, for some small enough constant c. Then, the discrete problem (4) has a unique solution $(\underline{u}_h, \underline{p}_h) \in \mathcal{V}_h$.*
Assume that the solution u of (1)-(2) is in $H^2(\Omega)\cap H_0^1(\Omega)$, and $u_k = u_{|\Omega^k} \in H^{2+m}(\Omega^k)$, with $M-1 \geq m \geq 0$. Let $p_{k,\ell} = \nu\frac{\partial u}{\partial \boldsymbol{n}_k} - \frac{\boldsymbol{a}\cdot\boldsymbol{n}_k}{2}u$ on $\Gamma^{k,\ell}$. Then, there exists a constant c independent of h and α such that

$$\|\underline{u}_h - \underline{u}\|_* + \|\underline{p}_h - \underline{p}\|_{-\frac{1}{2},*} \leq c(\alpha h^{2+m} + h^{1+m})\sum_{k=1}^{K}\|\underline{u}\|_{H^{2+m}(\Omega^k)} + c(\frac{h^m}{\alpha} + h^{1+m})\sum_{k=1}^{K}\sum_{\ell}\|p_{k,\ell}\|_{H^{\frac{1}{2}+m}(\Gamma^{k,\ell})}. \tag{5}$$

Moreover, if $p_{k,\ell} = \nu\frac{\partial u}{\partial \boldsymbol{n}_k} - \frac{\boldsymbol{a}\cdot\boldsymbol{n}_k}{2}u$ is in $H^{\frac{3}{2}+m}(\Gamma_{k,\ell})$, with $M-1 \geq m \geq 0$, then there exists c independent of h and α such that

$$\|\underline{u}_h - \underline{u}\|_* + \|\underline{p}_h - \underline{p}\|_{-\frac{1}{2},*} \leq c(\alpha h^{2+m} + h^{1+m})\sum_{k=1}^{K}\|\underline{u}\|_{H^{2+m}(\Omega^k)} + c(\frac{h^{1+m}}{\alpha} + h^{2+m})|\log h|\sum_{k=1}^{K}\sum_{\ell}\|p_{k,\ell}\|_{H^{\frac{3}{2}+m}(\Gamma^{k,\ell})} \tag{6}$$

5 Discrete iterative algorithm

The discrete algorithm to solve problem (4) is defined as follows : let $(u_{h,k}^n, p_{h,k}^n) \in X_h^k \times \tilde{W}_h^k$ be a discrete approximation of (u,p) in Ω^k at step n. Then, $(u_{h,k}^{n+1}, p_{h,k}^{n+1})$ is the solution in $X_h^k \times \tilde{W}_h^k$ of

$$\int_{\Omega^k}\left(\nu\nabla u_{h,k}^{n+1}\nabla v_{h,k} + (\eta + \frac{1}{2}\nabla\cdot\boldsymbol{a})u_{h,k}^{n+1}v_{h,k} + \frac{1}{2}\big((\boldsymbol{a}\cdot\nabla u_{h,k}^{n+1})v_{h,k} - (\boldsymbol{a}\cdot\nabla v_{h,k})u_{h,k}^{n+1}\big)\right)dx - \int_{\partial\Omega^k} p_{h,k}^{n+1}v_{h,k}ds = \int_{\Omega^k} f_k v_{h,k}dx,\ \forall v_{h,k} \in X_h^k, \tag{7}$$

$$\int_{\Gamma^{k,\ell}}(p_{h,k}^{n+1} + \alpha u_{h,k}^{n+1})\psi_{h,k,\ell} = \int_{\Gamma^{k,\ell}}(-p_{h,\ell}^{n} + \alpha u_{h,\ell}^{n})\psi_{h,k,\ell}, \quad \forall\psi_{h,k,\ell} \in \tilde{W}_h^{k,\ell}. \tag{8}$$

Using Lemma 2 in Japhet et al. [2013], we can prove the convergence of the iterative scheme

Theorem 2. *Under the hypothesis of Theorem 1, the algorithm (7)-(8) is well posed and converges in the sense that*

$$\lim_{n\longrightarrow\infty}(\|u_{h,k}^n - u_{h,k}\|_{H^1(\Omega^k)} + \sum_{\ell\neq k}\|p_{h,k,\ell}^n - p_{h,k,\ell}\|_{H_*^{-\frac{1}{2}}(\Gamma^{k,\ell})}) = 0,\ 1 \leq k \leq K.$$

6 Numerical results

We consider a P_1 finite element approximation. We study the numerical error analysis for problem (4). We consider the initial problem with exact solution $u(x,y) = x^3y^2 + sin(xy)$, $\eta = 1$ and $\nu = 0.01$. The domain is the unit square $\Omega = (0,1) \times (0,1)$. We decompose Ω into two non-overlapping subdomains with meshes generated in an independent manner as shown on Fig. 1.

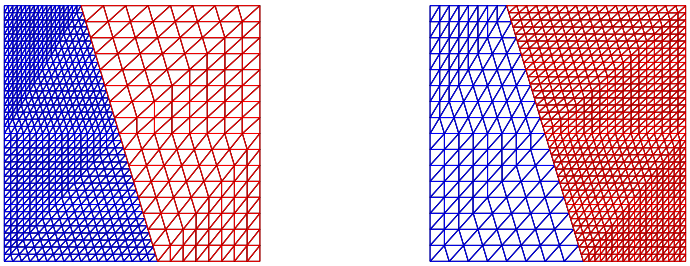

Fig. 1 Non-conforming meshes: mesh 2 (on the left), and mesh 3 (on the right)

The subdomain problems are solved using a direct solver. To observe the numerical error estimates for the discrete problem (4), one need to compute the converged solution of the algorithm (7)-(8) regardless of the algorithm used to compute it. Thus it is the solution at convergence of the algorithm (7)-(8) with a stopping criterion on the residual (i.e. the jumps of Robin conditions) that must be extremely small, e.g. smaller than 10^{-14}. The Robin parameter α is obtained by minimizing the convergence factor (see Japhet [1998], Dubois [2007]). For cases 1 and 2 below, this criterion is reached with an average of 40 and 45 iterations respectively (note that with Ventcell conditions, the number of iterations is almost independent of h (see Japhet et al. [2014]) and is 20 (case 1) and 26 (case 2). The error curves with Ventcell conditions are almost the same as the one on Fig.2 and Fig.3). Note that the regularity of the normal derivative of u along the interfaces enters most of the times in the frame of the error estimate (6) that allows a larger range of choice for α, compatible with the above chosen optimized choice.

Case 1. In this test case we have considered a rotating velocity defined by: $\boldsymbol{a} = (-\sin(\pi(y-\frac{1}{2}))\cos(\pi(x-\frac{1}{2})), \cos(\pi(y-\frac{1}{2}))\sin(\pi(x-\frac{1}{2})))$, and four initial meshes : meshes 1 to 4 where meshes 2 and 3 are the nonconforming meshes shown on Fig. 1, and mesh 1 (resp. mesh 4) is a conforming mesh obtained as the union of the coarse (resp. fine) sub-meshes of mesh 2 and mesh 3. Figure 2 shows the relative H^1 error versus the number of refinement for these four meshes, and the mesh size h versus the number of refinement, in logarithmic scale. At each refinement, the mesh size is divided by two. The results of Figure 2 show that the relative H^1 error tends to zero at the same

rate than the mesh size, and this fits with the theoretical error estimates of Theorem 1. On the other hand, we observe that the two curves corresponding to the non-conforming meshes (meshes 2 and 3) are between the curves of the conforming meshes (meshes 1 and 4). The relative H^1 error for mesh 3 is smaller than the one corresponding to mesh 2, and this is because mesh 3 is more refined than mesh 2 in the subdomain where the solution steeply varies.

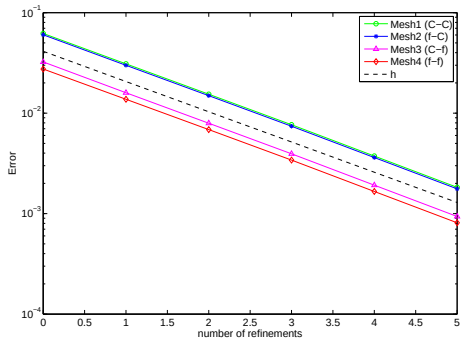

Fig. 2 Case 1. Relative H^1 error versus refinements for meshes 1-4.

Case 2. We consider a velocity built up from sets of vortices such that their closest neighbors rotate in the opposite directions (Smolarkiewicz [1982]), as shown on Fig. 3 (left) : $\boldsymbol{a} = 0.32\pi\,(\sin(4\pi x)\sin(4\pi y), \cos(4\pi y)\cos(4\pi x))\,.$

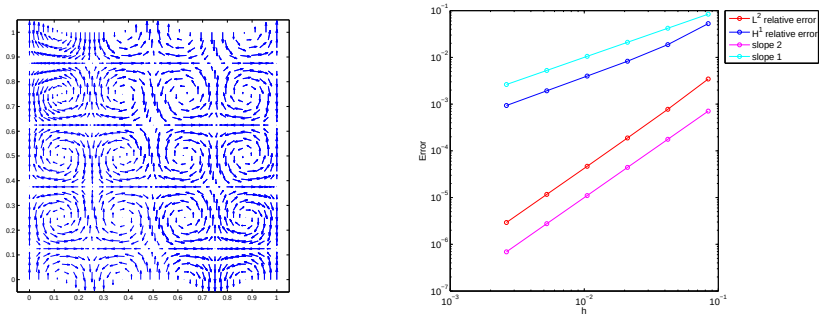

Fig. 3 Case 2. Left: velocity field. Right: Relative H^1 and L^2 errors versus h for mesh 3.

On Fig. 3 (right) we plot the relative H^1 error and the relative L^2 error versus the mesh size h, in logarithmic scale. We start from mesh 3 of Fig. 1 and then refine successively each mesh by dividing the mesh size by two. The results show that the relative H^1 (resp. L^2) error tends to zero at the same rate as the mesh size h (resp. h^2).

References

Y. Achdou, G. Abdoulaev, J.C. Hontand, Y.A. Kuznetsov, O. Pironneau, and C. Prud'homme. Nonmatching grids for fluids. In C. Farhat J. Mandel and X-C Cai, editors, *Domain decomposition methods 10*, pages 3–22. Contemporary Mathematics, 1998.

F. Ben Belgacem and Y. Maday. Coupling spectral and finite elements for second order elliptic three-dimensional equations. *SIAM J. Numer. Anal.*, 36(4):1234–1263, 1999.

C. Bernardi, Y. Maday, and A. T. Patera. A new nonconforming approach to domain decomposition: the mortar element method. In *Nonlinear partial differential equations and their applications. Collège de France Seminar, Vol. XI (Paris, 1989–1991)*, volume 299 of *Pitman Res. Notes Math. Ser.*, pages 13–51. Longman Sci. Tech., Harlow, 1994.

D. Braess and W. Dahmen. Stability estimates of the mortar finite element method for 3-dimensional problems. *East-West J. Numer. Math.*, 6(4): 249–263, 1998.

O. Dubois. Optimized schwarz methods with robin conditions for the advection-diffusion equation. In *Domain decomposition methods in science and engineering XVI*, volume 55 of *Lect. Notes Comput. Sci. Eng.*, pages 181–188. Springer, Berlin, 2007.

M. J. Gander, C. Japhet, Y. Maday, and F. Nataf. A new cement to glue nonconforming grids with Robin interface conditions: the finite element case. In *Domain decomposition methods in science and engineering*, volume 40 of *Lect. Notes Comput. Sci. Eng.*, pages 259–266. Springer, Berlin, 2005.

C. Japhet. Optimized Krylov-Ventcell method. Application to convection-diffusion problems. In U. Bjørstad, M. Espedal, and D.E. Keyes, editors, *Domain Decomposition Methods 9, Domain Decomposition Methods in Sciences and Engineering*, pages 382–389. John Wiley & Sons Ltd, 1998.

C. Japhet, Y. Maday, and F. Nataf. A New Interface Cement Equilibrated Mortar (NICEM) method with Robin interface conditions : the P_1 finite element case. *M3AS*, 23(12):2253–2292, 2013.

C. Japhet, Y. Maday, and F. Nataf. A new interface cement equilibrated mortar method with Ventcel conditions. In J. Erhel, M.J. Gander, L. Halpern, G. Pichot, T. Sassi, and O. Widlund, editors, *Domain decomposition methods in science and engineering XXI, Lecture Notes in Computational Science and Engineering*, volume 98, pages 329–336. Springer, 2014.

J.-L. Lions and E. Magenes. *Problèmes aux limites non-homogènes*, volume 1. Dunod, Paris, 1968.

P.K. Smolarkiewicz. The multi-dimensional crowley advection scheme. *Monthly Weather Review*, 110:1968–1983, 1982.